


Comparison of Critical Current Scaling Behaviors in MgB₂/SiC/Si Thin Films

Akihiko Nishida¹  · Chihiro Taka¹ ·
Stefan Chromik² · Rudolf Durny³

Received: 14 July 2016 / Accepted: 25 March 2017 / Published online: 6 April 2017
© Springer Science+Business Media New York 2017

Abstract Scaling behaviors of critical current density J_c in MgB₂ thin films are investigated on different films with thickness of 100 nm, in comparison with 50- and 10-nm films based on a comprehensive scaling formula. Experimental data are reduced and analyzed with the formula over a wide range of magnitudes. In 100- and 50-nm films the single scaling function has been able to fit experimental J_c data up to *ten orders of magnitudes* with appropriate flux pinning parameters. On the other hand, for the 10-nm film, different J_c dependences were found on temperature and magnetic field, concerning anomalous or granular superconductivity.

Keywords MgB₂ · Critical current · Scaling behavior

1 Introduction

Investigations of superconducting critical current density and its scaling behaviors are important, because the scaling behavior depends on the basic mechanism of superconductivity as well as the technical character of flux pinning.

In our previous article [1], we studied scaling behaviors of 50- and 10-nm MgB₂ thin films and showed that a single scaling formula is able to fit the critical current

✉ Akihiko Nishida
nishida@cis.fukuoka-u.ac.jp

¹ Department of Applied Physics, Fukuoka University, 8-19-1 Nanakuma, Jonan-ku, Fukuoka 814-0180, Japan

² Institute of Electrical Engineering, Slovak Academy of Sciences, Dubravská cesta 9, 841 04 Bratislava, Slovak Republic

³ Department of Physics, Slovak University of Technology, Ilkovicova 3, 812 19 Bratislava, Slovak Republic

density in 50-nm film for more than ten orders of magnitudes. On the other hand, for the 10-nm film, experimental data of the reduced current density indicated a kink in the middle temperature and field range, and fitting with the scaling formula was poor, suggesting weak pinning and anomalous superconductivity.

In this work, we investigate critical scaling behaviors of a 100-nm MgB₂ thin film and compare them with a similar scaling formula [1], on the basis of experimental results on the temperature dependence of the upper critical field, critical current density and irreversibility field as a function of reduced temperature as well as analyses on reduced critical current density as a function of reduced combination parameter of field and temperature.

In the absence of thermal activation of flux pinning, the critical current density J_c at temperature T and magnetic field H is expressed as

$$J_c(H, T) = A\mu_0^{m-1} H_{c2}^{m-\gamma}(T) H^{\gamma-1} [1-H/H_{c2}(T)]^\delta, \quad (1)$$

where A is a constant, $H_{c2}(T)$ is the upper critical field, and m , γ and δ are parameters depending on the flux pinning mechanism [2]. This is known as the scaling law with the empirical temperature dependence of $H_{c2}(T) = H_{c2}(0)[1 - (T/T_c)^2]$.

On the other hand, in the presence of thermally activated motion of fluxoids (flux creep), superconductors cannot carry non-resistive transport current outside the irreversibility line. The criterion is given by the irreversibility field $H_{irr}(T)$. Matsushita et al. [3] deduced an expression for $H_{irr}(T)$ appropriate for high- T_c superconductors (in which H_{irr} is much smaller than H_{c2}) as

$$H_{irr}(T) = (K/T)^p [1-(T/T_c)^2]^n, \quad (2)$$

where K is a constant determined by the electric field criterion of irreversibility and indices p and n are

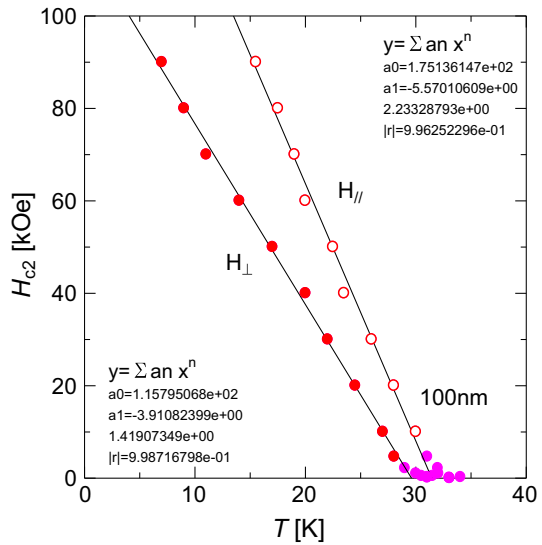
$$p = 4/(3-2\gamma), n = 2(m-\gamma)/(3-2\gamma). \quad (3)$$

However, it is reported that MgB₂ is not a regular high- T_c superconductor, and from the point of view of relaxation, it is much more a conventional superconductor, where H_{irr} does not differ much from H_{c2} [4].

2 Experimental

The MgB₂ film with 100 nm thickness studied here is the same film as in our previous report [5], which was prepared by sequential evaporation of boron and magnesium on an SiC-buffered Si substrate followed by in situ annealing. AC and DC magnetizations were measured using a PPMS magnetometer (Quantum Design). The upper critical field H_{c2} was estimated from AC susceptibility measurements with magnetic fields parallel and perpendicular to the film, while the critical current density J_c was evaluated from DC magnetization hysteresis under perpendicular magnetic field with the Bean critical state model: J_c [A/cm²] = $30\Delta M/r$, where ΔM [emu/cm³] is the height of the magnetization loop and r [cm] is the disk radius (about 0.16 cm).

Fig. 1 Upper critical field H_{c2} for 100-nm film under perpendicular (*solid circles*) and parallel (*open circles*) fields (Color figure online)



3 Results and discussion

The temperature dependence of the upper critical field H_{c2} in the 100-nm film is shown in Fig. 1 for parallel and perpendicular magnetic fields [5]. Least square fitting to the perpendicular data (*solid circles*) gives an estimation of $H_{c2}^{\perp}(0) = 116$ kOe, which will be used later as the upper critical field at 0 K for the 100-nm MgB₂ film.

It is noted here that in Fig. 1 $H_{c2}(T)$ shows practically a linear temperature dependence, while in Eq. (1) $H_{c2}(T) = H_{c2}(0)[1 - (T/T_c)^2]$ is assumed which should show a downward curvature at lowest temperatures. One possible explanation for the observed linearity comes from the fact that MgB₂ is a two-gap superconductor. It is reported that when π band electron scattering dominates over σ band scattering, the temperature dependence of H_{c2} becomes linear or even shows an upward curvature at lowest temperatures [6].

In Fig. 2, we present the critical current density J_c in the 100-nm MgB₂ film as a function of $1-t^2$ with $t = T/T_c$, ($T_c = 33.1$ K) at each value of constant magnetic field perpendicular to the film. Because of clarity, we here partially show our data for magnetic fields only below 1 kOe. The behavior is similar for magnetic fields above 1 kOe. As shown by solid lines in Fig. 2, the critical current density scales as $J_c(T) = J_c(0)[1 - (T/T_c)^2]^{m'}$.

The critical exponent m' estimated from least square fitting (solid lines) to J_c data is given in Fig. 3 as a function of magnetic field H . In a 50-nm film [1], the exponent m' increased monotonically from 4 at 0.1 kOe to 8 at 6.8 kOe. However, in the 100-nm film m' seems to oscillate between 3 and 7. Although the reason for such oscillation is not clear at present, some effects like matching field may concern.

The appearance of peaks in m' and concern of matching field can be further examined in Fig. 4, where J_c is shown as a function of magnetic field H at various temperatures [5]. Three peaks in Fig. 3 (around 0.5, 2 and 7 kOe) correspond to

Fig. 2 Variation of J_c as a function of $1-t^2$ with $t = T/T_c$ for 100-nm film. *Solid lines* indicate best linear fits to respective J_c at constant fields by $J_c(t) = J_c(0)(1-t^2)^{m'}$ (Color figure online)

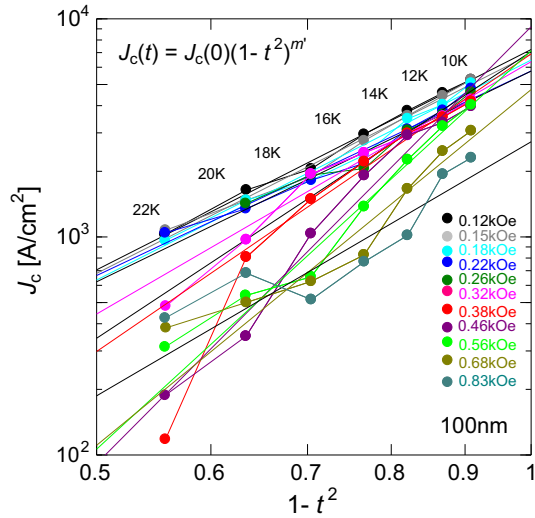
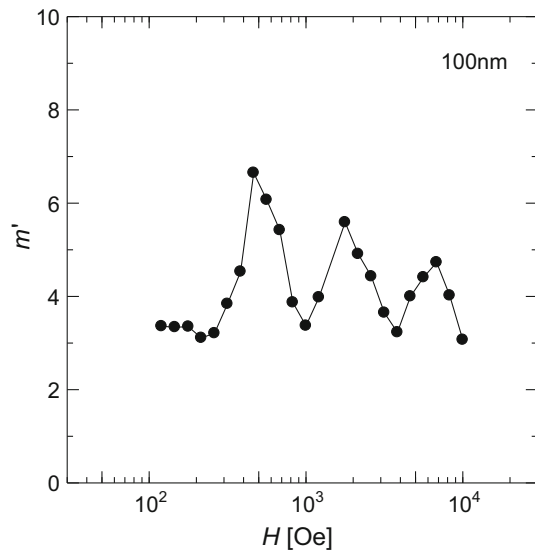


Fig. 3 Critical exponent m' oscillates between 3 and 7, suggesting some matching field effect



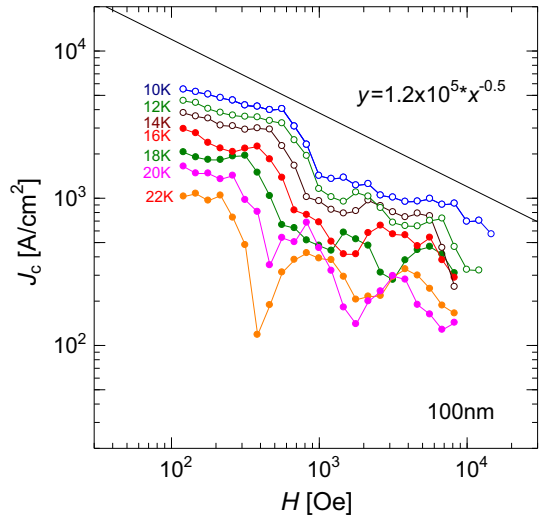
three minima in J_c observed at 20 and 22 K in Fig. 4. Although a matching field is generally expected to strengthen the flux pinning and enhance J_c , our case in Fig. 4 indicates somehow opposite effects, lowering J_c .

Finally, we are able to discuss the applicability of the theoretical Eq. (1) to our 100-nm MgB₂ film.

With the empirical temperature dependence of $H_{c2}(t) = H_{c2}(0)(1-t^2)$, Eq. (1) gives the scaling formula as

$$J_c(b_0, t) = J_\gamma b_0^{\gamma-1} (1-t^2)^{m-\gamma} [1-b_0/(1-t^2)]^\delta, \tag{4}$$

Fig. 4 Critical current density J_c in 100-nm MgB₂ film as a function of perpendicular magnetic field H (Color figure online)



where $J_\gamma = A\mu_0^{m-1}H_{c2}^{m-1}(0)$ and $b_0 = \mu_0 H / \mu_0 H_{c2}(0)$. When we compare this equation with the scaling formula of $J_c \sim (1-t^2)^{m'}$ in Fig. 2, we easily obtain the relationship of $m - \gamma = m'$, because the factor $1-b_0/(1-t^2)$ in Eq. (4) is not effective at lower fields like in Fig. 2 where $b_0 \ll 1$.

In order to examine the wide range of data with the single scaling formula for both temperature and magnetic field, Eq. (4) is finally transformed to

$$J_c(b_0, t) / (J_\gamma b_0^{m-1}) = ((1-t^2)/b_0)^{m-\gamma} [1-b_0/(1-t^2)]^\delta. \tag{5}$$

It should be noted that once the pinning parameters are given, the right-hand side of Eq. (5) contains no adjustable parameter.

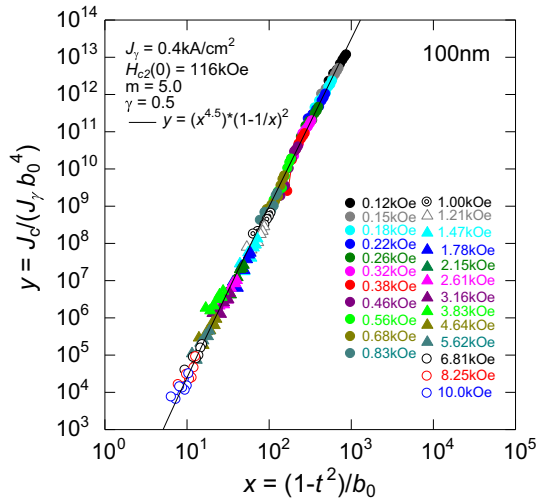
Therefore, we now examine various pinning parameters. As in our previous report [1], we first assume $\delta = 2$ according to literature [3,7] which corresponds to the presence of a saturation effect in the summation problem.

As also discussed previously [1], the intrinsic value of the critical exponent m' can be estimated from low field values in Fig. 3. However, being different from monotonous increase of m' with magnetic field in the 50-nm film [1], we here observe an oscillation of m' around 4.5 without any tendency of increase with magnetic field. We thus employ an estimation of $m' = 4.5$ (close to median of dispersion in Fig. 3).

The value of γ can be estimated from the magnetic field dependence of J_c at constant temperature low enough to neglect the flux creep effect. From Fig. 4, we can regard the field dependence of the critical current density at low temperatures as $J_c(H) \sim H^{-0.5}$. Comparing this dependence with Eq. (4), we obtain $\gamma - 1 = -0.5$, and thus γ is estimated to be 0.5, and then $m = m' + \gamma = 5.0$.

The estimation of $\gamma = 0.5$ is consistent with the flux pinning effect by normal inclusions such as Mg₂Si, MgO and C-substitution [8]. A larger value of $m = 5.0$ than the literature estimation of $m = 2.0$ in the powder MgB₂ [7] may indicate some additional effect of surface pinning with stronger temperature dependence.

Fig. 5 Plot of reduced critical current density $y = J_c/(J_\gamma b_0^{4.0})$ in 100-nm film as a function of $x = (1-t^2)/b_0$ with $b_0 = H/H_{c2}(0)$ (Color figure online)



Putting values of these pinning parameters as $m = 5.0$, $\gamma = 0.5$ and $\delta = 2.0$, we plot in Fig. 5 the experimental reduced critical current density $y = J_c/(J_\gamma b_0^{4.0})$ as a function of $x = (1 - t^2)/b_0$ under perpendicular magnetic field. Here, we employed $H_{c2}^\perp(0) = 116 \text{ kOe}$ according to Fig. 1. As remarkably can be seen, a wide range of experimental data in temperature from 10 to 22 K and in field from 0.1 to 10 kOe are aligned in a single line. Either larger or smaller m than 5.0 results in a gap among different sets of data (with different colors) for respective fields and deteriorates data alignment from the single line. This also supports the appropriateness of the values of $m = 5.0$ and $\gamma = 0.5$. All these pinning parameters are the same as in our previous 50-nm film [1].

The solid line in Fig. 5 represents Eq. (5) as $y = x^{4.5}(1-1/x)^2$, and the line fits experimental data very well over 9 orders of magnitude in reduced J_c . This is equally remarkable along with our 50-nm film, where fitting was successful over 10 orders of magnitudes [1]. On making such fit, the only adjustable parameter is the scaling factor J_γ which reflects the pinning strength through the factor $AH_{c2}^{m-1}(0)$ in Eq. (4), and the value of 0.4 kA/cm^2 results in the best agreement between experimental data and the scaling Eq. (5). This value of J_γ is three orders of magnitudes smaller than our 50-nm film. It is also noted that our analyses differ from the generally employed scaling method [3] in a sense that we use inverse variable $x = 1/b = (1-t^2)/b_0$ and that we explicitly treat the temperature dependence of H_{c2} .

We should again note that the scaling was good without need of taking into account thermal activation of vortices. This conclusion is in accord with the fact that MgB_2 exhibits only a weak relaxation and that MgB_2 is not a regular high- T_c superconductor, but it is much more a conventional superconductor [4].

We further examine the variation of the pinning parameters from film to film. First, the value of δ is fixed to 2 as mentioned above according to Ref. [3] and [7]. The value of m cannot be exactly determined in the 10-nm film because of a kink as shown in Fig. 4 in Ref. [1]. The value of $\gamma = -1.0$ in the 10-nm film is very anomalous and

probably reflects granular or amorphous nature of superconductivity as mentioned in Ref. [1] and [9]. As for 50- and 100-nm films, γ (and also m) takes the same value of 0.5 (and 5.0) with normal inclusions and surface pinning. J_γ in A/cm² varies like 20, 6×10^5 , 400 for 10-, 50-, 100-nm films, respectively. The very small value of J_γ in the 10-nm film also reflects granular nature of superconductivity. The largest J_γ value in the 50-nm film is probably due to good crystallinity with some additional effect of surface pinning. In order to further clarify the thickness effect on these pinning parameters, we need some more variation of thickness in MgB₂ films, such as 200 and 500 nm.

At high temperatures ($T \sim T_c$), Eq. (2) reduces to the well-known scaling relation for the irreversibility field:

$$H_{\text{irr}}(T) = H_{\text{irr}}(0)[1-(T/T_c)^2]^n, \quad (6)$$

According to Eq. (3) with the above pinning parameter values, the exponent n in Eq. (6) is expected to be 4.5. However, this does not agree with our previously observed value of $n = 8$ [5] in the scaling behavior of H_{irr} in 100-nm film. Although such discrepancy in the scaling exponent n for the irreversibility field also appeared in our 50-nm film [1], the observed value was smaller in the 50-nm film, while larger in the 100-nm film than 4.5. A larger value of n would probably be related to the smaller value of the pinning strength parameter J_γ in the 100-nm film. In fact, the observed maximum J_c is three orders of magnitudes smaller than that of 50-nm film.

In summary, scaling behaviors of J_c and H_{irr} in a 100-nm MgB₂ thin film are examined in comparison with our previous 50-nm film. Both scaling behaviors in 100- and 50-nm films are well explained by the model without flux creep effect over 9 or 10 orders of magnitude in the reduced J_c , which corresponds to good film quality and sound superconductivity in contrast to poor superconductivity in a 10-nm film [1, 9]. This conclusion is also in accord with the fact that bulk MgB₂ exhibits only a weak relaxation and that MgB₂ is not a regular high- T_c superconductor, but it is closer to a conventional superconductor [4]. However, the critical exponent in the scaling behavior of H_{irr} was larger in the 100-nm film, inferring weaker pinning strength than the 50-nm film with smaller exponent. With our results for J_c scaling behaviors in both films, it is fair to conclude that the theoretical scaling formula [Eq. (4)] is well applicable to J_c without flux creep effect and is useful to predict practical J_c values in various temperatures and fields.

Acknowledgements This work was supported in part by the Central Research Laboratory, Fukuoka University (Project #145004), and magnetic measurements were taken at the Advanced Materials Institute Facilities established at Fukuoka University under the support from the Ministry of Education, Culture, Sports, Science and Technology.

References

1. A. Nishida, C. Taka, S. Chromik, R. Durny, Phys. Proc. **36**, 644–648 (2012)
2. A.M. Campbell, J.E. Evetts, Adv. Phys. **21**, 199–428 (1972)
3. T. Matsushita, T. Fujiyoshi, K. Toko, K. Yamafuji, Appl. Phys. Lett. **56**, 2039–2041 (1990)

4. M. Jirsa, M. Rames, M.R. Koblichka, A. Koblichka-Veneva, K. Berger, B. Douine, *Supercond. Sci. Technol.* **29**, 025006 (2016)
5. A. Nishida, C. Taka, S. Chromik, R. Durny, *J. Phys.: Conf. Ser.* **507**, 012036 (2014)
6. V. Braccini et al., *Phys. Rev. B* **71**, 012504 (2005)
7. K. Kitahara, T. Akune, Y. Matsumoto, N. Sakamoto, *Phys. C* **445–448**, 471–473 (2006)
8. S. Chromik, A. Nishida, V. Strbik, M. Gregor, J.P. Espinos, J. Liday, R. Durny, *Appl. Surf. Sci.* **269**, 29–32 (2013)
9. A. Nishida, C. Taka, S. Chromik, R. Durny, *Proceedings of ICEC23-ICMC2010*, Wrocław, Poland, pp. 1249–1254 (2011)